Supporting information for:

Fluorescence Analysis of the Lipid Binding-induced Conformational Change of Apolipoprotein E4

Chiharu Mizuguch, Mami Hata, Padmaja Dhanasekaran, Margaret Nickel, Michael C. Phillips, Sissel Lund-Katz, and Hiroyuki Saito

EXPERIMENTAL PROCEDURES

Proteins

The human apoE4 variants studied contained the mutations S94C, W264C or S290C so that a single cysteine residue was present in each molecule. Residue 94 is located in the N-terminal helix bundle domain whereas residues 264 and 290 are located in the C-terminal domain. These apoE4 variants were labeled with pyrene at the cysteine residue. Control experiments were conducted using wild-type (WT) human apoE4 and its monomeric form containing the mutations F257A/W264R/V269A/L279Q/V287E (*1*).

Circular Dichroism (CD) Spectroscopy

Far-UV CD spectra were recorded from 185 to 260 nm at 25 °C using a Jasco J-600 spectropolarimeter. The α-helix content was derived from the molar ellipticity at 222 nm, as described (*2*).

Gel Filtration Chromatography

The proteins were incubated at 0.25 mg/ml in 6 M GdnHCl (100 mM ammonium bicarbonate, 10 mM dithiothreitol (DTT), pH 8.1) for 16 h at 4 °C and dialyzed for 24 h at the same temperature against 10 mM Tris-buffered saline (TBS), pH 7.4 containing 1 mM DTT. The apoE concentration was then determined by A_{280} using a reference value calculated from the amino acid composition. In the case of pyrene-labeled samples, experimentally determined absorbances relative to Lowry protein values were used. A 1 ml aliquot of the apoE solution (typically containing 200-220 μg protein) was applied to two Superdex 200 columns (60 x 1.6 cm) connected in series and eluted at 1 ml/min with 10 mM TBS (no DTT present) using an Akta FPLC system. The elution of the apoE was monitored on-line via A_{280}; 2-4 independent experiments were performed for each apoE variant. The column (void volume = 91.5 ml and total volume = 236.4 ml) was calibrated using proteins of known diameter (nm) and mass (Da) as described before (*3*) so that these parameters for an apoE variant could be calculated from the K_{av} value using the following equations:

1) $\log_{10}(\text{mass}) = -2.74\, K_{av} + 6.25$

2) $\log_{10}(\text{diameter}) = -1.10\, K_{av} + 1.37$

For ^{14}C-labeled HDL experiments, a 1 ml aliquot of the trace ^{14}C-labeled HDL (lysine residues were methylated) in TBS (pH 7.4) before or after incubation of 10 μg/ml apoE4 for 30 min at room temperature was applied to the two Superdex 200 columns.

RESULTS

Effects of Cys Substitution on ApoE4 Structure

Far-UV CD spectra of apoE4 variants (Fig. S1A) demonstrated that all cysteine mutants have almost identical secondary structure: the α-helix contents for intact, S94C, W264C, and

S290C apoE4 were 48, 51, 49, and 52%, respectively. Fig. S1B shows GdnHCl denaturation curves for apoE4 variants monitored by the change in molar ellipticity at 222 nm. Although the apoE4 cysteine mutants displayed more monophasic-like denaturation curves than the WT protein which underwent biphasic denaturation (*4*), there was not much difference among all denaturation curves. These results indicate that the cysteine mutations used in this study do not significantly perturb the protein structure and stability of apoE4.

Effects of Cys Substitution and Pyrene Labeling on the Self-Association Behavior of ApoE4

Monomeric apoE4 elutes at an elution volume (V_e) of 159ml as a single peak with K_{av} = 0.47 (Fig. S2A), corresponding to an apparent molecular mass of 92 kDa and a hydrodynamic diameter of 7.1 nm. The molecular weight of this apoE4 variant in the same buffer was also determined independently by quasi-elastic light scattering and sedimentation velocity ultracentrifugation; the average molecular weight by these two methods was 34,000 (data not shown) which is the same as the formula weight confirming that the protein is indeed monomeric under the conditions studied. The fact that the apparent molecular mass calculated from the K_{av} is 92 kDa indicates that this apoE4 molecule is more expanded and/or asymmetric than the globular proteins used to calibrate the gel filtration column, presumably due to the influence of its more disordered, molten globule, helix bundle domain.

For the purpose of analysis of elution profiles of the cysteine-containing apoE variants, peaks with elution volumes of about 158 and 177 ml are considered to arise from apoE monomers whereas peaks at lower elution volumes are attributed to the existence of oligomeric apoE. It is well known that human apoE4 self-associates according to a monomer-dimer-tetramer process with the tetramer being predominant at micro-molar concentrations (*5*). Consistent with

this concept, apoE4 exhibits a major elution peak at 127 ml (Fig. S2B); the K_{av} corresponds to an apparent molecular mass of 391 kDa (diameter = 13 nm) reflecting the existence of tetramers (theoretical molecular mass = 136 kDa) that are presumably highly asymmetric. The peak at 159 ml arises from apoE4 in the monomeric state (expanded conformation).

The self-association behavior of the apoE4 S94C variant is shown in Figs. S3A and S3B. It is apparent that the mutation has little or no effect in apoE4 (cf. Figs. S2B and S3A). Addition of the pyrene label to apoE4 S94C does not affect tetramer formation (cf. Figs. S2B and S3B) but apparently shifts the monomer to the compact form (Fig. S3B).

Figs. S3C and S3D show equivalent elution profiles obtained for apoE4 variant containing the mutation W264C in the C-terminal domain. Comparison of the profiles in Fig. S3C and Fig. S2B demonstrates that this mutation does not prevent self-association but shifts the monomer-tetramer equilibrium towards the monomer state. Importantly, addition of pyrene to the cysteine residue at position 264 strongly inhibits apoE4 self-association (cf. Figs. S3C and S3D).

In order to be able to label the C-terminal domain of apoE4 without altering the self-association properties, the mutation S290C was introduced. As shown in Figs. S3E and S3F, neither the mutation nor addition of the pyrene label affects the oligomerization of apoE4. The presence of the pyrene label in apoE4 S290C induces adoption of the compact monomeric structure (V_e = 177 ml) rather than the expanded monomer structure (V_e = 159 ml).

Overall, the mutations S94C and S290C in human apoE4 are relatively non-perturbing in terms of the self-association behavior of the protein molecules. The gel filtration elution profiles for these apoE4 variants when pyrene-labeled are similar to their WT counterparts, in which apoE4 S290C-pyrene apparently adopts a compact monomer state (V_e = 179 ml; Fig. S3F). Consistent with our prior work showing that residues 261-272 are important for lipid-binding,

the attachment of pyrene at position 264 induces major perturbations of apoE4 self-association; tetramer formation is essentially eliminated in the case of apoE4 W264C-pyrene (Fig. S3D).

GdnHCl-induced Acrylodan Fluorescence Change of ApoE4 Variants

Fig. S4 shows the change in acrylodan fluorescence emission spectra of apoE4 W264C-Ac and S290C-Ac when incubated at different concentrations of GdnHCl. In contrast to apoE4 S94C-Ac (Fig. 1) and W264C-Ac (Fig. S4A), the acrylodan fluorescence intensity of apoE4 S290C-Ac increases at relatively low GdnHCl concentration (Fig. S4B) perhaps because self-quenching of acrylodan in close proximity occurs due to oligomerization of apoE4. Supporting this, the inflection point of change in acrylodan fluorescence intensity is close to that for pyrene excimer/monomer ratio of apoE4 S290C-pyrene (Fig. S4C).

Effect of SUV Binding to FRET in ApoE4 S94C-Ac

Compared to unlabeled apoE4 S94C, there were significant decreases in Trp emission fluorescence at around 340 nm and the concomitant appearance of an acrylodan fluorescence peak at around 480 nm in apoE4 S94C-Ac, indicating the occurrence of FRET from Trp residues to acrylodan in apoE4 (Fig. S5A). In contrast, upon binding to SUV, the difference in the Trp fluorescence between the unlabeled and acrylodan-labeled apoE4 S94C and acrylodan fluorescence peak became remarkably small (Fig. S5B), indicating decreases in FRET due to increased separation of the Trp residues and acrylodan. The similar dependency of FRET efficiency in apoE4 S94C-Ac and increase in pyrene fluorescence of apoE4 S94C-pyrene on the SUV interaction (Fig. S5C) indicates that the change in FRET mainly reflects the conformational

change of the N-terminal domain upon lipid binding, that is, the helix bundle opening of the N-terminal domain.

Gel Filtration of ^{14}C-labeled HDL

To check the possibility if the binding of apoE4 induces the displacement of HDL proteins, gel filtration chromatography of ^{14}C-labeled HDL was conducted. As shown in Fig. S6, HDL elutes as two peaks between 120−170 ml with the main peak at 138 ml. Since lipid-free apoA-I eluted with a peak at 166 ml (data not shown), it is apparent that there is no free ^{14}C-apoA-I in the preparation. Co-incubation of ^{14}C-HDL with apoE4 resulted in the identical elution profiles, indicating that apoE4 did not displace any HDL proteins.

REFERENCES

1. Zhang, Y., S. Vasudevan, R. Sojitrawala, W. Zhao, C. Cui, C. Xu, D. Fan, Y. Newhouse, R. Balestra, W. G. Jerome, K. Weisgraber, Q. Li, and J. Wang. 2007. A monomeric, biologically active, full-length human apolipoprotein E. *Biochemistry* **46**: 10722-10732.

2. Sakamoto, T., Tanaka, M., Vedhachalam, C., Nickel, M., Nguyen, D., Dhanasekaran, P., Phillips, M. C., Lund-Katz, S., and Saito, H. 2008. Contributions of the carboxyl-terminal helical segment to the self-association and lipoprotein preferences of human apolipoprotein E3 and E4 isoforms, *Biochemistry* **47**: 2968-2977.

3. Liu, L., A. E. Bortnick, M. Nickel, P. Dhanasekaran, P. V. Subbaiah, S. Lund-Katz, G. H. Rothblat, and M. C. Phillips. 2003. Effects of apolipoprotein A-I on ATP-binding cassette

transporter A1-mediated efflux of macrophage phospholipid and cholesterol. *J.Biol.Chem.* **278**: 42976-42984.

4. Tanaka, M., Vedhachalam, C., Sakamoto, T., Dhanasekaran, P., Phillips, M. C., Lund-Katz, S., and Saito, H. 2006: Effect of carboxyl-terminal truncation on structure and lipid interaction of human apolipoprotein E4, *Biochemistry* **45**: 4240-4247.

5. Garai, K., and C. Frieden. 2010. The association-dissociation behavior of the ApoE proteins: kinetic and equilibrium studies. *Biochemistry* **49**: 9533-9541.

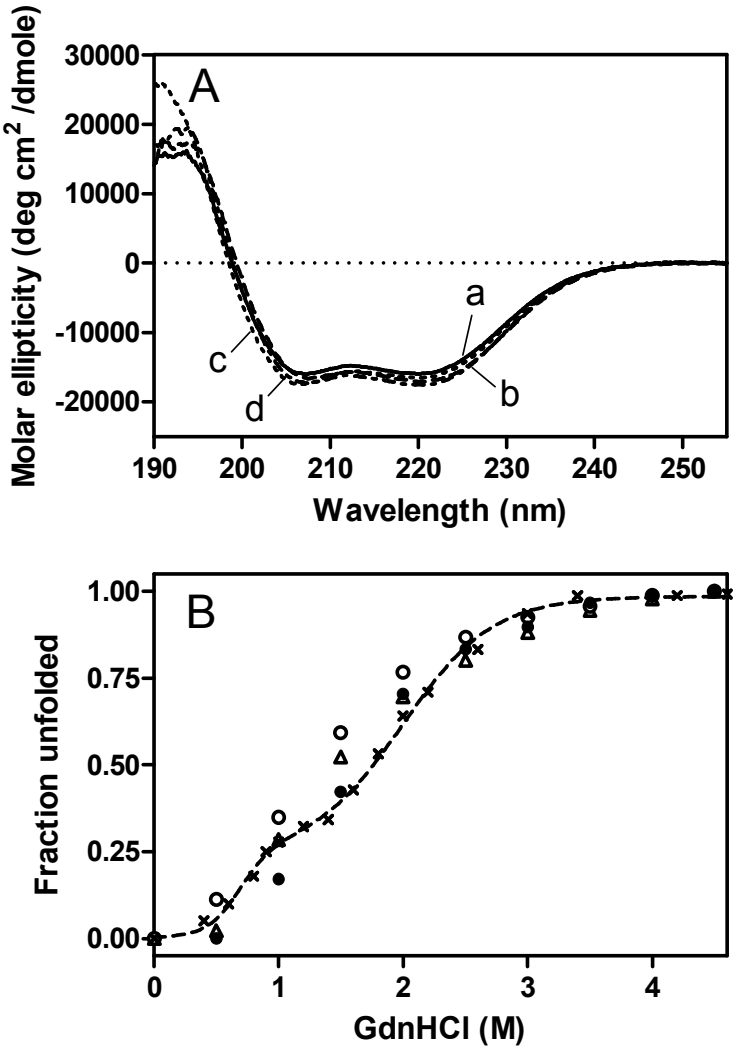

Fig. S1: Far-UV CD spectra (A) and GdnHCl denaturation curves (B) of apoE4 variants. *A*, apoE4 (a), apoE4 S94C (b), apoE4 W264C (c), and apoE4 S290C (d). Protein concentration was 50 μg/ml. *B*, GdnHCl denaturation curves monitored by CD. Δ, apoE4 S94C; ○, apoE4 W264C; ●, apoE4 S290C; ×, apoE4. Protein concentration was 25 μg/ml.

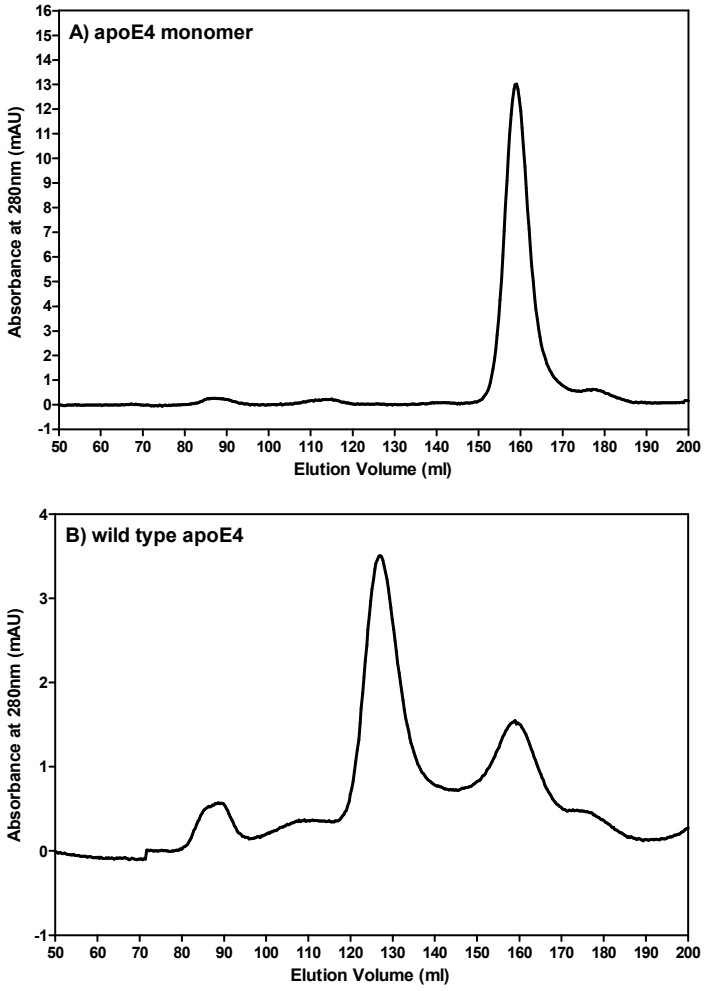

Fig. S2: Gel filtration profiles of wild-type apoE4 and its monomeric variant.

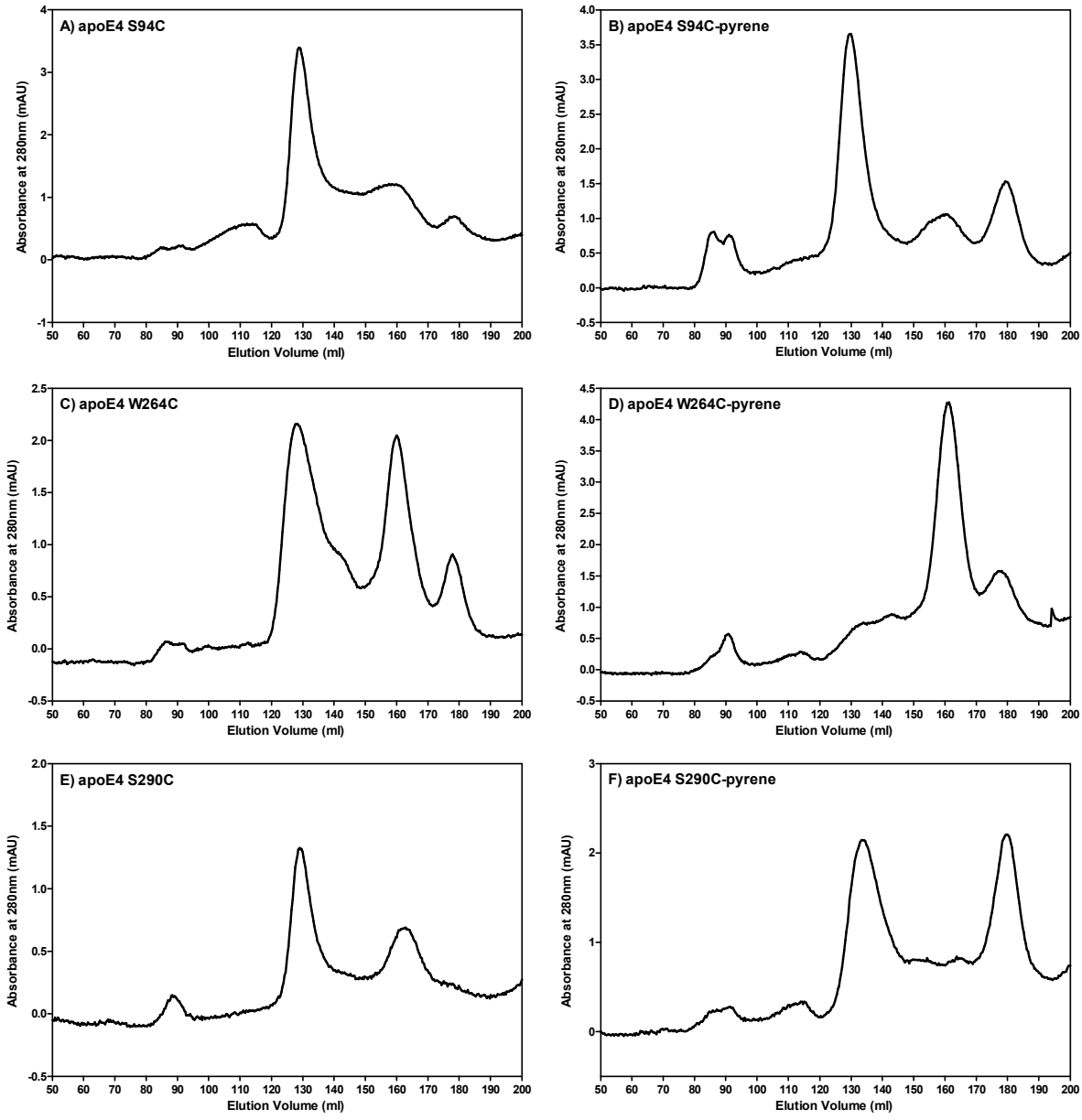

Fig. S3: Gel filtration profiles of apoE4 S94C, W264C, and S290C variants without and with pyrene labeling.

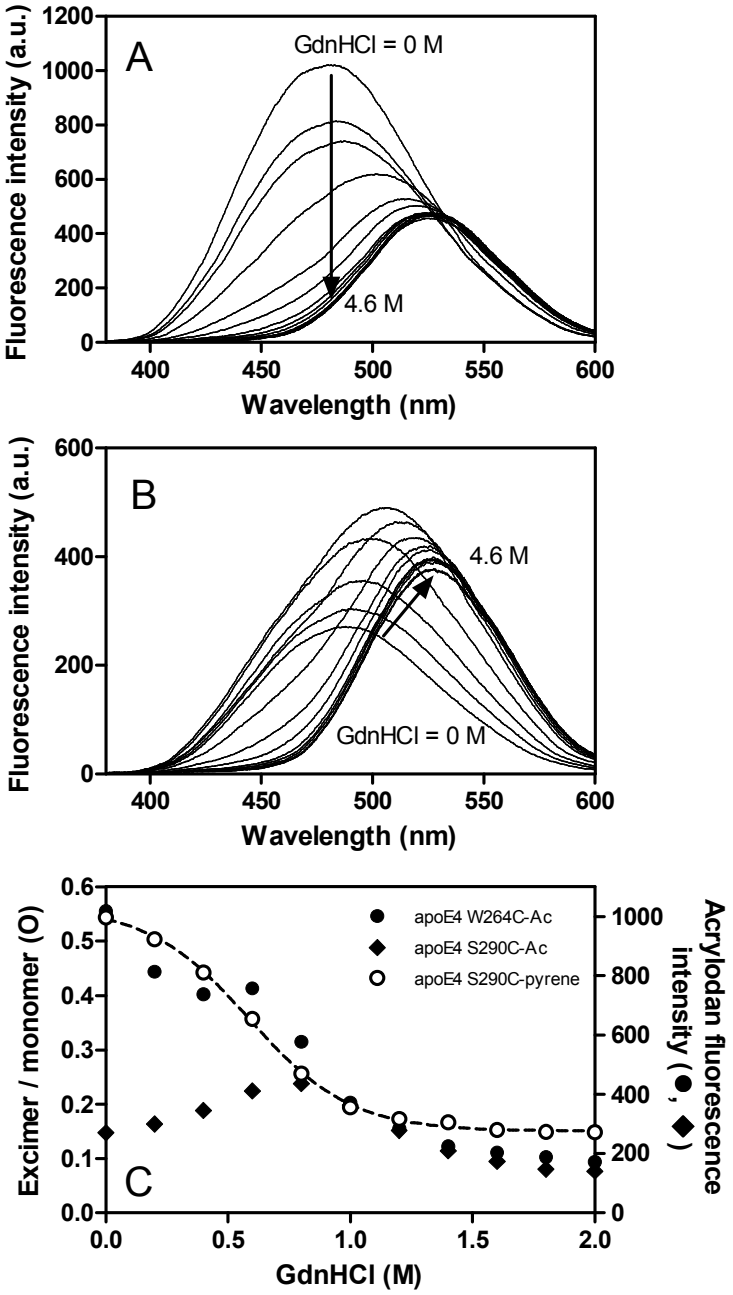

Fig. S4: Acrylodan fluorescence emission spectra of apoE4 W264C-Ac (A) and S290C-Ac (B) at different concentrations of GdnHCl (from 0 to 4.6 M). (C) The change in acrylodan fluorescence intensity for apoE4 W264C-Ac (●) and S290C-Ac (♦), and excimer/monomer ratio of pyrene fluorescence for apoE4 S290C-pyrene (○) as a function of GdnHCl concentration.

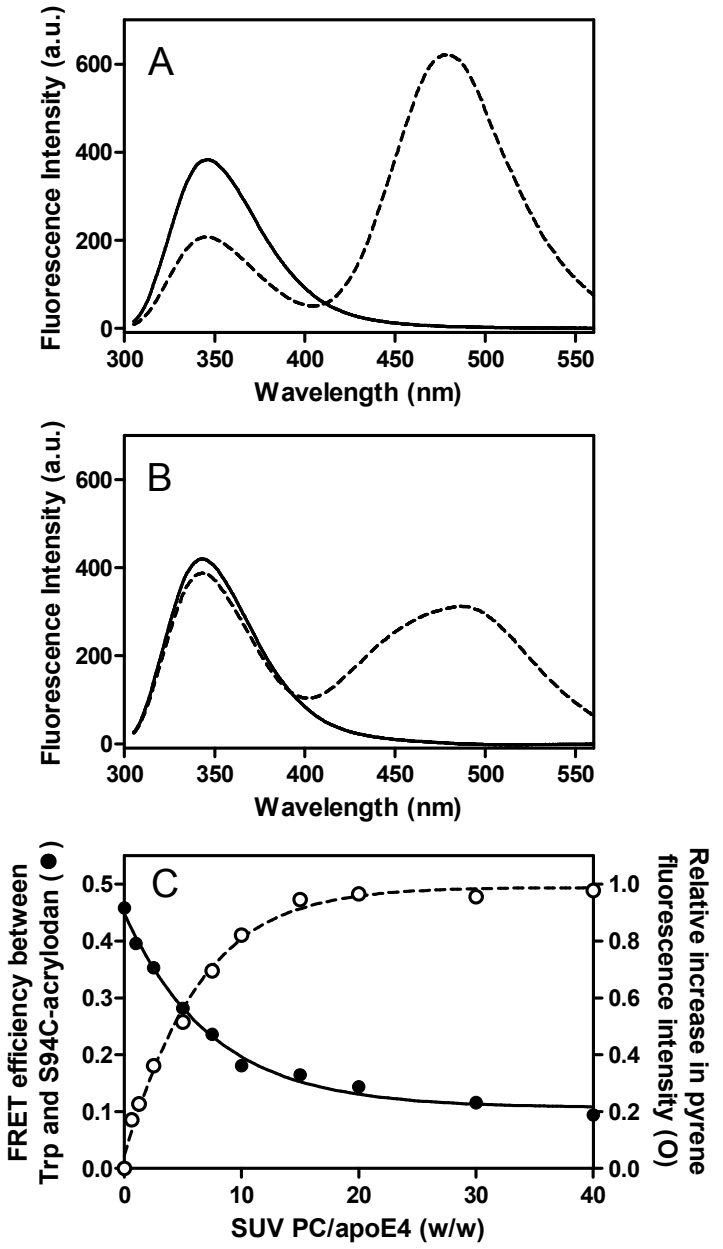

Fig. S5: FRET between Trp residues and acrylodan in apoE4 S94C-acrylodan. Fluorescence emission spectra excited at 290 nm for unlabeled (solid line) and acrylodan-labeled (dashed line) apoE4 S94C were recorded in the lipid-free (A) or SUV-bound (B) states. Protein and PC concentrations were 25 μg/ml and 1.0 mg/ml, respectively. (C) The change in FRET efficiency for apoE4 S94C-Ac (●) and increase in pyrene fluorescence for apoE4 S94C-pyrene (○) as a function of the weight ratio of PC to apoE4.

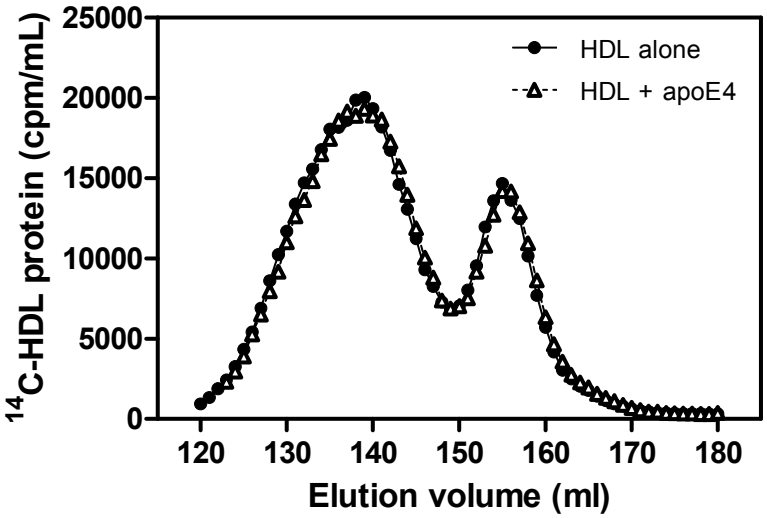

Fig. S6: Gel filtration elution profiles of ^{14}C-labeled HDL (0.4 mg protein/ml) before (●) or after (Δ) incubation of apoE4 (10 μg/ml).